NNLO QCD predictions for the LHC with antenna subtraction

João Pires (MPI Munich)

Les Houches Workshop, Physics at the TeV colliders
June 7, 2017

Max-Planck-Institut für Physik
(Werner-Heisenberg-Institut)

MAX-PLANCK-GESELLSCHAFT

Anatomy of an NNLO calculation

$$
\begin{aligned}
d\hat{\sigma}_{NNLO} = & \int_{d\Phi_4} d\hat{\sigma}^{RR}_{NNLO} \\
& + \int_{d\Phi_3} d\hat{\sigma}^{RV}_{NNLO} \\
& + \int_{d\Phi_2} d\hat{\sigma}^{VV}_{NNLO}
\end{aligned}
$$

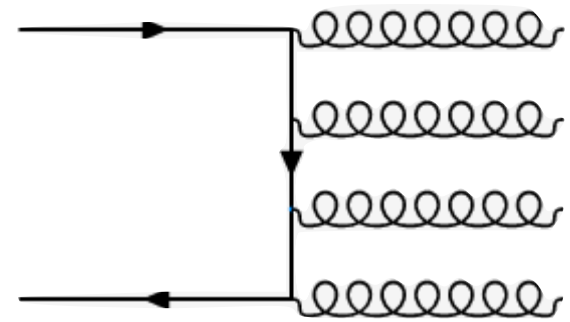

- double-unresolved
- single-unresolved

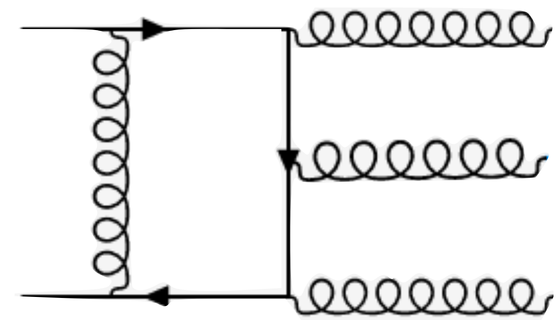

- single-unresolved
- $1/\varepsilon^2$; $1/\varepsilon$

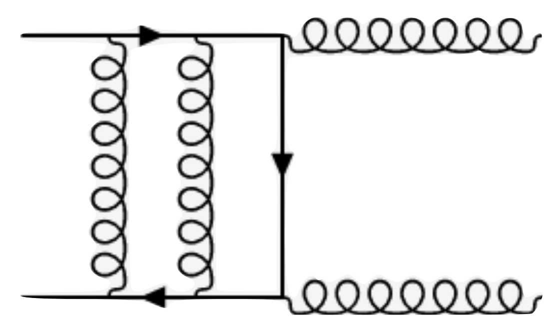

- $1/\varepsilon^4$; $1/\varepsilon^3$; $1/\varepsilon^2$; $1/\varepsilon$;

Assume all matrix elements are available

- Tree level matrix elements (RR) $2 \rightarrow n+2$
- One-loop matrix elements (RV) $2 \rightarrow n+1$

Form NLO correction to 2->n+1

- Two loop matrix elements (VV) $2 \rightarrow n$

Infrared singularities: real radiation

NLO

- single collinear: $p_a \,//\, p_b$
- single soft: $E_a \to 0$

NNLO

- Triple collinear: $p_a \,//\, p_b \,//\, p_c$
- Double single collinear: $p_a \,//\, p_b$; $p_c \,//\, p_d$
- Soft/collinear: $E_a \to 0$, $p_b \,//\, p_c$
- Double soft: $E_a \to 0$, $E_b \to 0$
- One-loop virtual correction to NLO singularities

NNLO antenna subtraction

$$
\begin{aligned}
d\hat{\sigma}_{NNLO} \quad &= \int_{d\Phi_4} \left(d\hat{\sigma}^{RR}_{NNLO} - d\hat{\sigma}^{S}_{NNLO} \right) \\
&+ \int_{d\Phi_3} \left(d\hat{\sigma}^{RV}_{NNLO} - d\hat{\sigma}^{T}_{NNLO} \right) \\
&+ \int_{d\Phi_2} \left(d\hat{\sigma}^{VV}_{NNLO} - d\hat{\sigma}^{U}_{NNLO} \right)
\end{aligned}
$$

$d\hat{\sigma}^{S}_{NNLO} \quad d\hat{\sigma}^{T}_{NNLO}$

- mimic RR,RV in unresolved limits

$d\hat{\sigma}^{T}_{NNLO} \quad d\hat{\sigma}^{U}_{NNLO}$

- analytically cancel the poles in RV and VV matrix elements

- NNLO cross section with each line finite and integrable in d=4 dimensions

Implementation in parton-level event generator

- Generate particle momenta for (n), (n+1), (n+2)
- Reconstruct observable
- Weight with squared matrix elements
- Subtract/add real radiation singularities

Colour ordering

- QCD amplitudes in colour basis

All gluon

$$\mathcal{A}_n^{\text{tree}}(\{k_i, \lambda_i, a_i\}) = g^{n-2} \sum_{\sigma \in S_n/Z_n} \text{Tr}\left(T^{a_{\sigma(1)}} \cdots T^{a_{\sigma(n)}}\right) A_n^{\text{tree}}(\sigma(1^{\lambda_1}), \ldots, \sigma(n^{\lambda_n}))$$

Quark pair plus gluons

$$\mathcal{A}_n^{\text{tree}} = g^{n-2} \sum_{\sigma \in S_{n-2}} \left(T^{a_{\sigma(3)}} \cdots T^{a_{\sigma(n)}}\right)_{i_2}^{\bar{\jmath}_1} A_n^{\text{tree}}(1_{\bar{q}}^{\lambda_1}, 2_q^{\lambda_2}, \sigma(3^{\lambda_3}), \ldots, \sigma(n^{\lambda_n}))$$

- Real radiation infrared singularities only between colour adjacent partons

- Well defined patterns from colour-connections

Antenna subtraction at NNLO (RR)

$$\mathrm{d}\sigma^{S}_{NNLO} = \mathrm{d}\sigma^{S,a}_{NNLO} + \mathrm{d}\sigma^{S,b}_{NNLO} + \mathrm{d}\sigma^{S,c}_{NNLO} + \mathrm{d}\sigma^{S,d}_{NNLO} + \mathrm{d}\sigma^{S,e}_{NNLO}$$

- (a) one unresolved parton → three parton antenna function X_{ijk}
- (b) two colour-connected unresolved partons → four parton antenna function X_{ijkl}

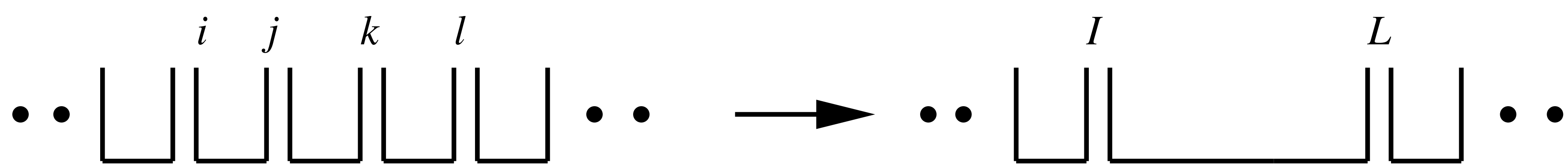

- (c) two almost colour connected unresolved partons → strongly ordered product of non-independent three parton antenna functions $X_{ijk}X_{Klm}$, $X_{klm}X_{ijK}$

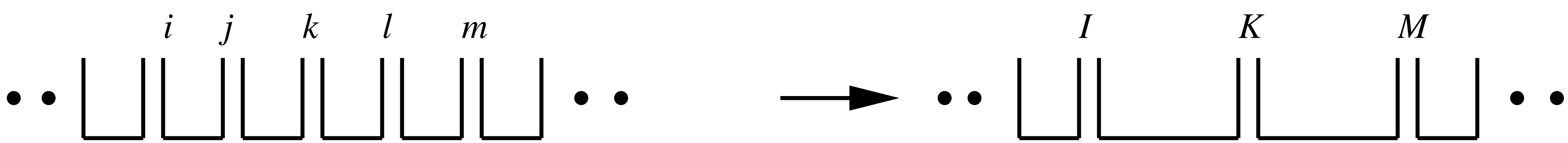

- (d) two colour unconnected unresolved partons → product of independent three parton antenna functions $X_{ijk}X_{nop}$

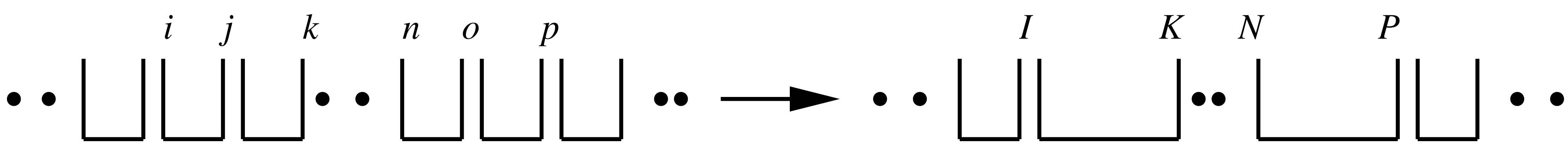

- (e) subtracts large angle soft radiation → soft factor S_{ajc}

Two colour connected partons

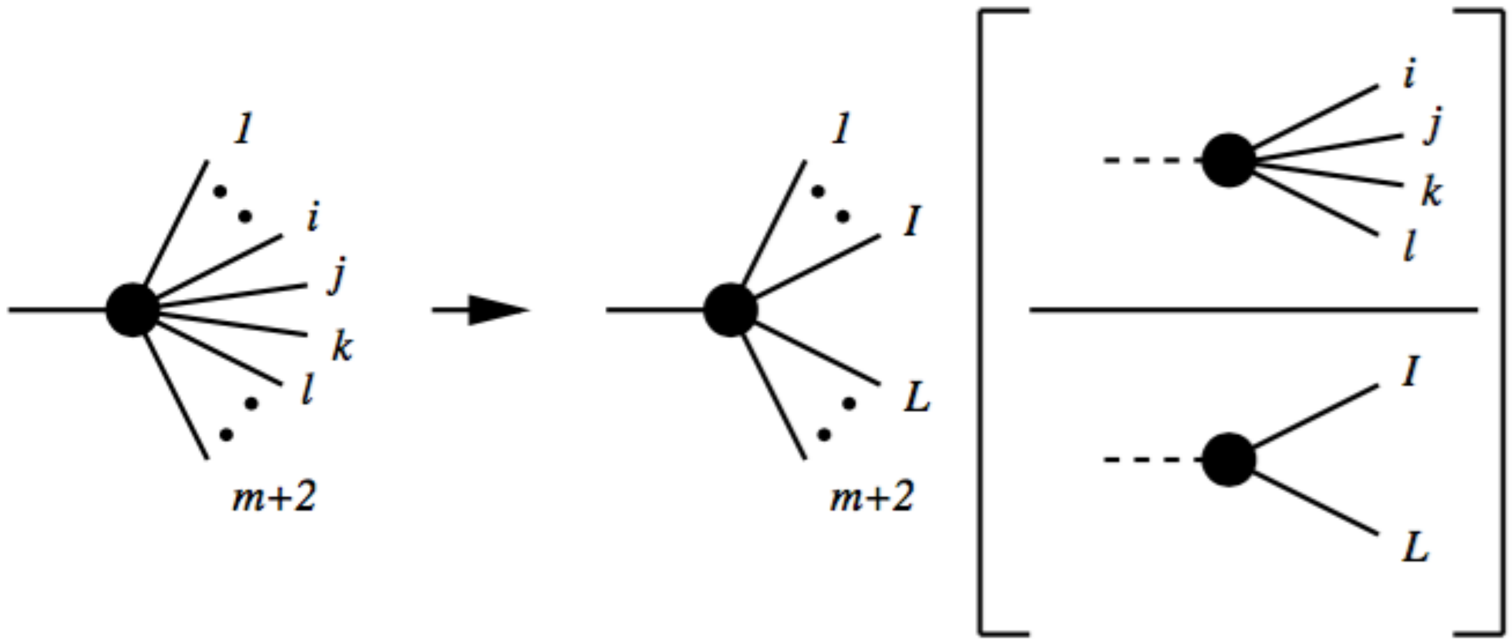

Four-parton antenna function

$$d\sigma_{NNLO}^{S,b} = \mathcal{N} \sum_{m+2} d\Phi_{m+2}(p_1, \ldots, p_{m+2}; q) \frac{1}{S_{m+2}}$$
$$\times \left[\sum_{jk} \left(X_{ijkl}^0 - X_{ijk}^0 X_{IKl}^0 - X_{jkl}^0 X_{iJL}^0 \right) \right.$$
$$\left. \times \, |\mathcal{M}_m(p_1, \ldots, \tilde{p}_I, \tilde{p}_L, \ldots, p_{m+2})|^2 \, J_m^{(m)}(p_1, \ldots, \tilde{p}_I, \tilde{p}_L, \ldots, p_{m+2}) \right],$$

$$A_4^0(i_q, j_g, k_g, l_{\bar{q}}) \xrightarrow{E_j,\, E_k \to 0} S_{ijkl}$$

$$A_4^0(i_q, j_g, k_g, l_{\bar{q}}) \xrightarrow{p_i // p_j // p_k} P_{qgg \to Q}(w, x, y)$$

$$A_4^0(i_q, j_g, k_g, l_{\bar{q}}) \xrightarrow{E_k \to 0,\, p_i // p_j} S_{q;gg\bar{q}} P_{qg \to Q}(z)$$

$$A_4^0(i_q, j_g, k_g, l_{\bar{q}}) \xrightarrow{p_i // p_j;\, p_k // p_l} P_{qg \to Q}(z) P_{\bar{q}g \to \bar{Q}}(y)$$

smoothly interpolates
colour connected
unresolved limits

- Phase space mapping (i,j,k,l)→(I,L)

$$p_I = xp_i + r_1 p_j + r_2 p_k + z p_l$$

$$p_L = (1-x)p_i + (1-r_1)p_j + (1-r_2)p_k + (1-z)p_l$$

$$\begin{aligned}
x = & \frac{1}{2(s_{12}+s_{13}+s_{14})}\Big[(1+\rho)\, s_{1234} \\
& -r_1\,(s_{23}+2\,s_{24}) - r_2\,(s_{23}+2\,s_{34}) \\
& +(r_1-r_2)\frac{s_{12}s_{34}-s_{13}s_{24}}{s_{14}}\Big] \\
z = & \frac{1}{2(s_{14}+s_{24}+s_{34})}\Big[(1-\rho)\, s_{1234} \\
& -r_1\,(s_{23}+2\,s_{12}) - r_2\,(s_{23}+2\,s_{13}) \\
& -(r_1-r_2)\frac{s_{12}s_{34}-s_{13}s_{24}}{s_{14}}\Big] \\
\rho = & \Big[1+\frac{(r_1-r_2)^2}{s_{14}^2\, s_{1234}^2}\,\lambda(s_{12}\,s_{34}, s_{14}\,s_{23}, s_{13}\,s_{24}) \\
& +\frac{1}{s_{14}\,s_{1234}}\Big\{2\,(r_1\,(1-r_2)+r_2(1-r_1))(s_{12}s_{34}+s_{13}s_{24}-s_{23}s_{14}) \\
& \qquad +4\,r_1\,(1-r_1)\,s_{12}s_{24}+4\,r_2\,(1-r_2)\,s_{13}s_{34}\Big\}\Big]^{\frac{1}{2}},
\end{aligned}$$

$$r_1 = \frac{s_{23}+s_{24}}{s_{12}+s_{23}+s_{24}}$$

$$r_2 = \frac{s_{34}}{s_{13}+s_{23}+s_{34}}$$

$$\mathrm{d}\Phi_{m+2}(p_1,\ldots,p_{m+2}) = \mathrm{d}\Phi_m(p_1,\ldots,p_I,p_L,\ldots,p_{m+2})\cdot \mathrm{d}\Phi_{X_{ijkl}}(p_i,p_j,p_k,p_l;p_I,p_L)$$

$$\{p_i, p_j, p_k, p_l\} \to \{p_I, p_L\}$$

$$\xrightarrow{E_j, E_k \to 0} \quad p_I = p_i, \quad p_L = p_l$$

$$\xrightarrow{p_i // p_j // p_k} \quad p_I = p_i + p_j + p_k, \quad p_L = p_l$$

$$\xrightarrow{E_k \to 0,\, p_i // p_j} \quad p_I = p_i + p_j, \quad p_L = p_l$$

$$\xrightarrow{p_i // p_j;\, p_k // p_l} \quad p_I = p_i + p_j, \quad p_L = p_k + p_l$$

smoothly interpolates
colour connected
unresolved limits

Antenna functions and types

- all antennae can be derived from physical matrix elements in QCD
- colour ordered pair of hard partons (radiators) with radiation in between
  - hard quark-antiquark pair
  - hard quark-gluon pair
  - hard gluon-gluon pair
- three parton antennae → one unresolved parton
- four-parton antennae → two unresolved partons
- can be at tree level or one loop
- can be massless or massive
- all have three antenna types
  - final-final antenna
  - initial-final antenna
  - initial-initial antenna

$$\boxed{X_3^0(i,j,k)}$$

$$\boxed{X_4^0(i,j,k,l)}$$

$$\boxed{X_3^1(i,j,k)}$$

Angular averaging

- Antenna functions are scalar objects → do not subtract angular correlations in gluon splitting

- Angular correlations vanish after integration over the azimuthal angle

$$\frac{1}{2\pi}\int_0^{2\pi} \mathrm{d}\phi\,(p_l\cdot k_\perp) = 0\,, \qquad \frac{1}{2\pi}\int_0^{2\pi} \mathrm{d}\phi\,(p_l\cdot k_\perp)^2 = -k_\perp^2\,\frac{p\cdot p_l\, n\cdot p_l}{p\cdot n}$$

$$\Theta_{F_3^0}(i,j,z,k_\perp) \sim A\cos(2\phi+\alpha)$$

- Make fully local subtraction by combining phase space points related to each other by a 90 degree rotation of the system of unresolved partons

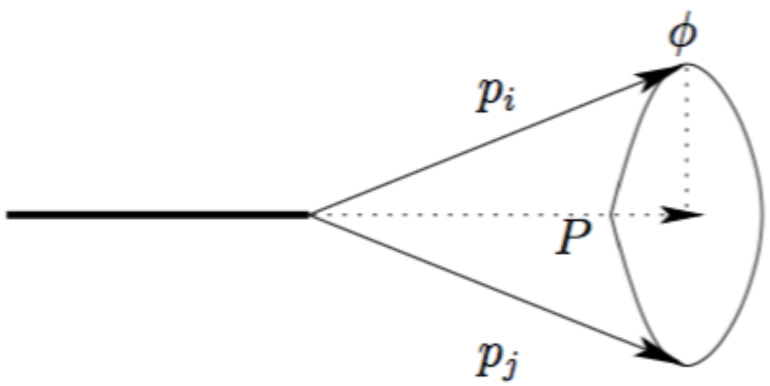

$$p_i^\mu = zp^\mu + k_\perp^\mu - \frac{k_\perp^2}{z}\frac{n^\mu}{2p\cdot n}\,, \qquad p_j^\mu = (1-z)p^\mu - k_\perp^\mu - \frac{k_\perp^2}{1-z}\frac{n^\mu}{2p\cdot n}\,,$$

with $2p_i\cdot p_j = -\dfrac{k_\perp^2}{z(1-z)}\,,\qquad p^2 = n^2 = k_\perp.p = k_\perp.n = 0$

Antenna subtraction at work

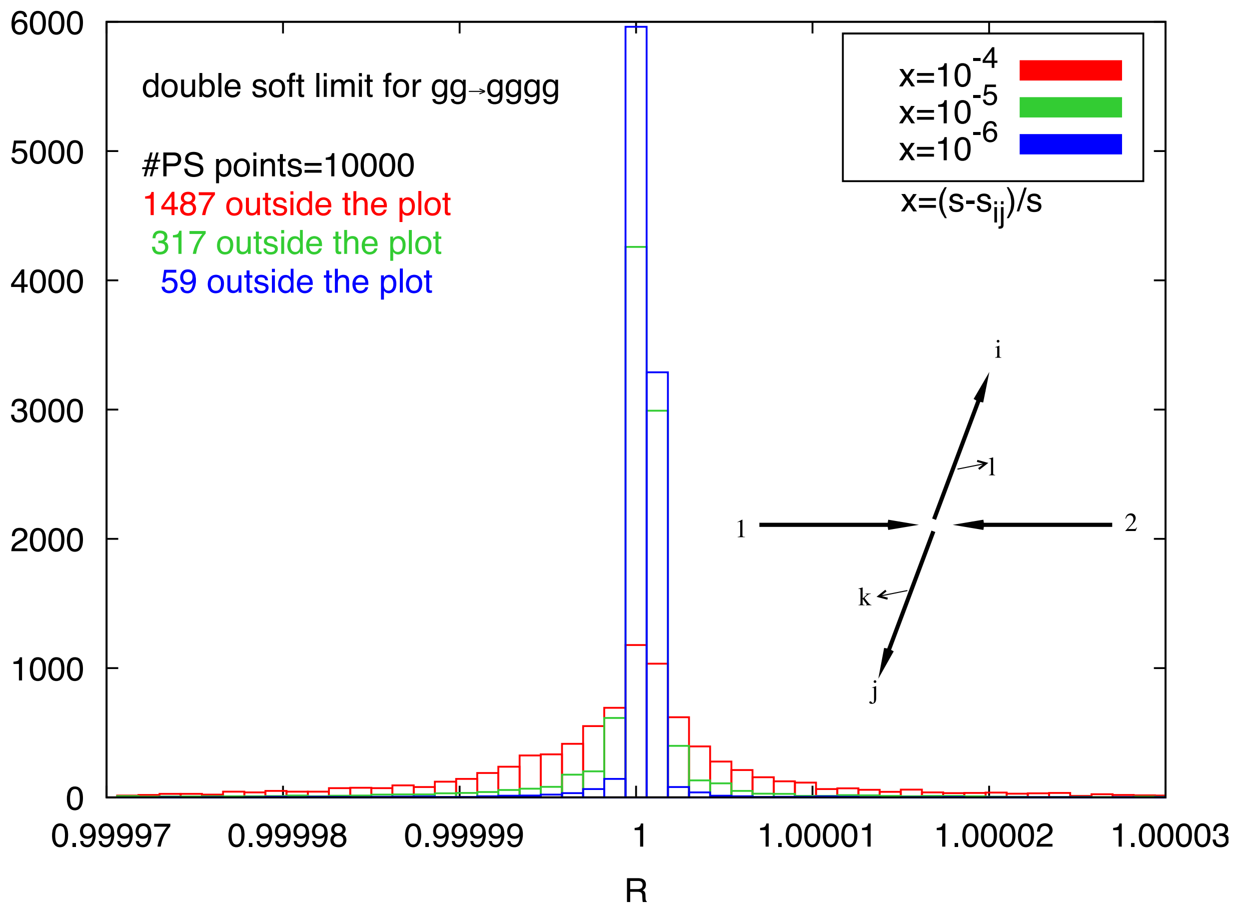

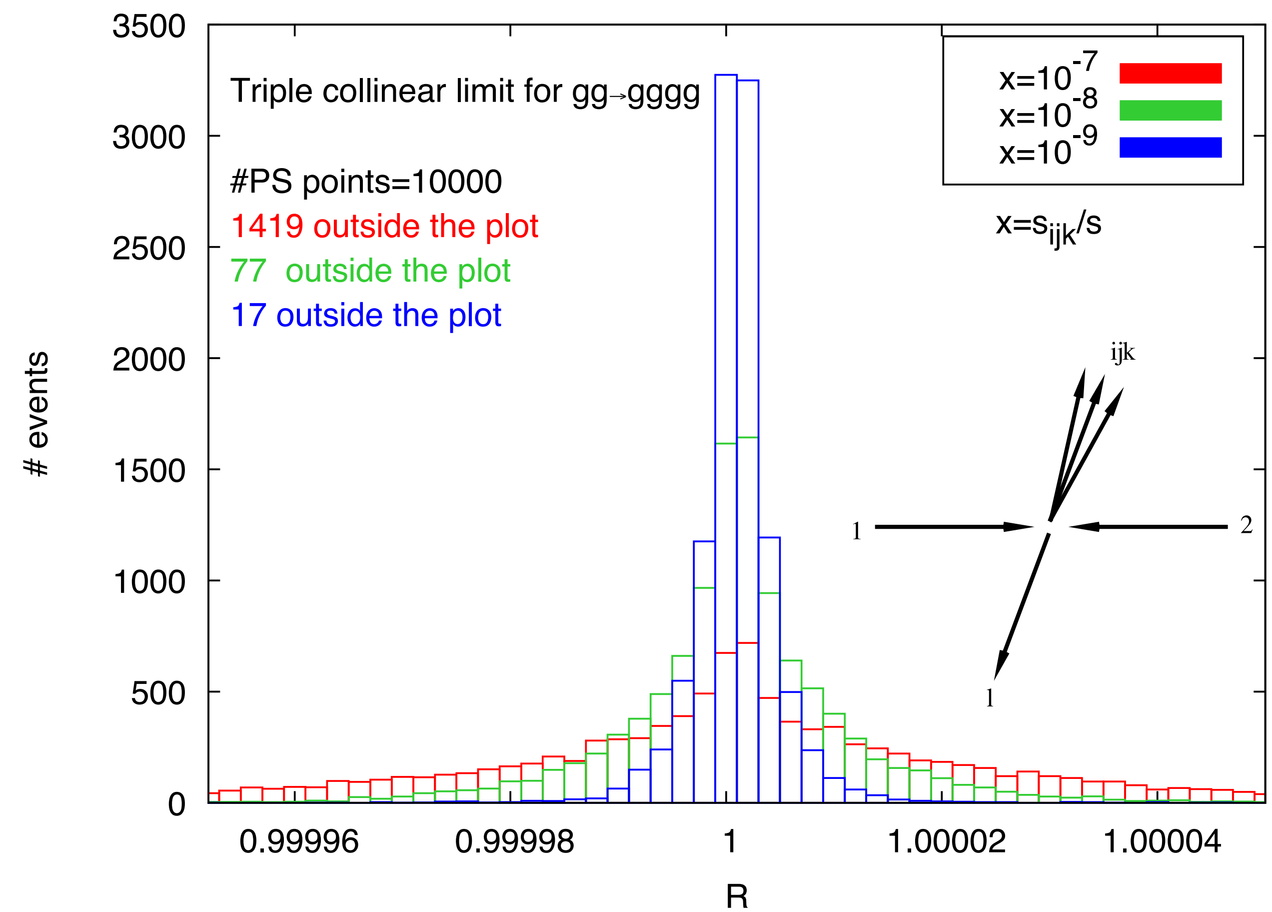

Double unresolved emission

- Generate phase space trajectories that approach singular region of the phase space
- Infrared behaviour of subtraction term mimics the behaviour of the matrix element

$$R = \frac{d\sigma^R_{NNLO}}{d\sigma^S_{NNLO}} \xrightarrow{l_g, k_g \to 0} 1$$

Double virtual antenna contribution

	a	b	b,c	d	e
$\mathrm{d}\hat{\sigma}^{S}_{NNLO}$	$X_3^0\lvert\mathcal{M}^0_{m+3}\rvert^2$	$X_4^0\lvert\mathcal{M}^0_{m+2}\rvert^2$	$X_3^0 X_3^0\lvert\mathcal{M}^0_{m+2}\rvert^2$	$X_3^0 X_3^0\lvert\mathcal{M}^0_{m+2}\rvert^2$	$\mathcal{S}X_3^0\lvert\mathcal{M}^0_{m+2}\rvert^2$
$\int_1 \mathrm{d}\hat{\sigma}^{S,1}_{NNLO}$	$\mathcal{X}_3^0\lvert\mathcal{M}^0_{m+3}\rvert^2$	–	$\mathcal{X}_3^0 X_3^0\lvert\mathcal{M}^0_{m+2}\rvert^2$	–	$\mathcal{S}X_3^0\lvert\mathcal{M}^0_{m+2}\rvert^2$
$\int_2 \mathrm{d}\hat{\sigma}^{S,2}_{NNLO}$	–	$\mathcal{X}_4^0\lvert\mathcal{M}^0_{m+2}\rvert^2$	–	$\mathcal{X}_3^0 \mathcal{X}_3^0\lvert\mathcal{M}^0_{m+2}\rvert^2$	–

- Integrated double unresolved emission of RR process ∝ tree level double soft function
- Integrated iterated NLO emissions of RR process

- Integrated single unresolved emission from RV process ∝ tree level single soft function
- Integrated single unresolved emission of RV process ∝ one loop single soft function

	$\mathrm{d}\hat{\sigma}^{T}_{NNLO}$		
Final State Particles	a	a	(b,c)
$m+1$	$X_3^1\lvert\mathcal{M}^0_{m+2}\rvert^2$	$X_3^0\lvert\mathcal{M}^1_{m+2}\rvert^2$	$\mathcal{X}_3^0 X_3^0\lvert\mathcal{M}^0_{m+2}\rvert^2$
m	$\mathcal{X}_3^1\lvert\mathcal{M}^0_{m+2}\rvert^2$	$\mathcal{X}_3^0\lvert\mathcal{M}^1_{m+2}\rvert^2$	$\mathcal{X}_3^0 \mathcal{X}_3^0\lvert\mathcal{M}^0_{m+2}\rvert^2$

Double virtual antenna contribution

	a	b	b,c	d	e
$\mathrm{d}\hat{\sigma}^{S}_{NNLO}$	$X_3^0\lvert\mathcal{M}^0_{m+3}\rvert^2$	$X_4^0\lvert\mathcal{M}^0_{m+2}\rvert^2$	$X_3^0 X_3^0\lvert\mathcal{M}^0_{m+2}\rvert^2$	$X_3^0 X_3^0\lvert\mathcal{M}^0_{m+2}\rvert^2$	$SX_3^0\lvert\mathcal{M}^0_{m+2}\rvert^2$
$\int_1 \mathrm{d}\hat{\sigma}^{S,1}_{NNLO}$	$\mathcal{X}_3^0\lvert\mathcal{M}^0_{m+3}\rvert^2$	–	$\mathcal{X}_3^0 X_3^0\lvert\mathcal{M}^0_{m+2}\rvert^2$	–	$\mathcal{S}X_3^0\lvert\mathcal{M}^0_{m+2}\rvert^2$
$\int_2 \mathrm{d}\hat{\sigma}^{S,2}_{NNLO}$	–	$\mathcal{X}_4^0\lvert\mathcal{M}^0_{m+2}\rvert^2$	–	$\mathcal{X}_3^0 \mathcal{X}_3^0\lvert\mathcal{M}^0_{m+2}\rvert^2$	–

$$\mathcal{P}oles(\mathrm{d}\hat{\sigma}^{U,a}_{NNLO}) \quad \sim \quad \mathbf{J^1}(\epsilon,\hat{1}_g,\hat{2}_g,i_g,j_g)\Big(A_4^1(\hat{\hat{1}}_g,\hat{\hat{2}}_g,i_g,j_g)-\frac{b_0}{\epsilon}A_4^0(\hat{\hat{1}}_g,\hat{\hat{2}}_g,i_g,j_g)\Big)$$

$$\mathcal{P}oles(\mathrm{d}\hat{\sigma}^{U,b}_{NNLO}) \quad \sim \quad \mathbf{J^1}(\epsilon,\hat{1}_g,\hat{2}_g,i_g,j_g)\otimes\mathbf{J^1}(\epsilon,\hat{1}_g,\hat{2}_g,i_g,j_g)A_4^0(\hat{\hat{1}}_g,\hat{\hat{2}}_g,i_g,j_g)$$

$$\mathcal{P}oles(\mathrm{d}\hat{\sigma}^{U,c}_{NNLO}) \quad \sim \quad \mathbf{J^2}(\epsilon,\hat{1}_g,\hat{2}_g,i_g,j_g)\,A_4^0(\hat{\hat{1}}_g,\hat{\hat{2}}_g,i_g,j_g)$$

	$\mathrm{d}\hat{\sigma}^{T}_{NNLO}$		
Final State Particles	a	a	(b,c)
$m+1$	$X_3^1\lvert\mathcal{M}^0_{m+2}\rvert^2$	$X_3^0\lvert\mathcal{M}^1_{m+2}\rvert^2$	$\mathcal{X}_3^0 X_3^0\lvert\mathcal{M}^0_{m+2}\rvert^2$
m	$\mathcal{X}_3^1\lvert\mathcal{M}^0_{m+2}\rvert^2$	$\mathcal{X}_3^0\lvert\mathcal{M}^1_{m+2}\rvert^2$	$\mathcal{X}_3^0 \mathcal{X}_3^0\lvert\mathcal{M}^0_{m+2}\rvert^2$

- integrated operators $\mathbf{J}_2^{(2,1)}$ in analytic one-to-one correspondence with $(\mathbf{I}_1)^2$ operator of Catani

$$
\begin{aligned}
d\sigma_{VV} &= 2\boldsymbol{I}^{(1)}(\epsilon, \hat{1}_g, \hat{2}_g, i_g, j_g)\, A_4^1(\hat{1}_g, \hat{2}_g, i_g, j_g) \\
&- 2\boldsymbol{I}^{(1)}(\epsilon, \hat{1}_g, \hat{2}_g, i_g, j_g)^2\, A_4^0(\hat{1}_g, \hat{2}_g, i_g, j_g) \\
&+ \boldsymbol{I}^{(2)}(\epsilon, \hat{1}_g, \hat{2}_g, i_g, j_g)) \\
&+ \text{Finite}(A_2^2(\hat{1}_g, \hat{2}_g, i_g, j_g))
\end{aligned}
$$

$$
\begin{aligned}
d\sigma_{U} &= \mathbf{J}_4^1(1_g, 2_g, i_g, j_g) A_4^1(1_g, 2_g, i_g, j_g) \\
&+ \frac{1}{2}\mathbf{J}_4^1(1_g, 2_g, i_g, j_g) \otimes \mathbf{J}_4^1(1_g, 2_g, i_g, j_g) A_4^0(1_g, 2_g, i_g, j_g) \\
&+ \mathbf{J}_4^2(1_g, 2_g, i_g, j_g) A_4^0(1_g, 2_g, i_g, j_g)
\end{aligned}
$$

```
[Joaos-MacBook-Pro:jet pires$ form autoA4g2XU.frm
FORM 4.1 (Oct 25 2013) 64-bits                      Run: Sun Apr  9 17:19:06 2017
    #-

   poles = 0;

  32.20 sec out of 32.54 sec
```

$$
\boxed{\mathcal{P}oles\left(\mathrm{d}\hat{\sigma}^{VV}_{NNLO} - \mathrm{d}\hat{\sigma}^{U}_{NNLO}\right) = 0}
$$

Pros and cons

Antenna subtraction

- local method with phase space averaging → good control on the numerical accuracy of the final result, RR, RV, VV separately finite
- analytic IR pole cancellation at NNLO → good control on the correctness of the pole cancellation
- double precision
- universal method works for general jet multiplicity → no additional building blocks needed
- pp→jj,Hj,Zj @ NNLO
- subtraction terms for a fixed colour structure reusable
- involves many mappings/subtraction terms as expected for a local method → needs caching system to store mappings

NNLOJET parton level generator

[X. Chen, J. Cruz-Martinez, J.Currie, A. Gehrmann-De Ridder, T. Gehrmann, N. Glover, A. Huss, M.Jaquier, T.Morgan, J. Niehues, JP]

- parton level generator based on antenna subtraction to compute fully differential cross sections at NNLO in QCD
- all antenna functions implemented with a common syntax and structure
- allows testing of matrix element/subtraction term cancellations with singular phase space trajectories
- allows explicit 1/e pole cancelation with one and two loop matrix elements with FORM
- interface to phase space generation, Monte Carlo integration and fully flexible histograming
- interface to applfast nnlo tables in development

M. Sutton and K. Rabbertz tomorrow afternoon

NNLOJET parton level generator

[X. Chen, J. Cruz-Martinez, J.Currie, A. Gehrmann-De Ridder, T. Gehrmann,
N. Glover, A. Huss, M.Jaquier, T.Morgan, J. Niehues, JP]

- list of processes available in NNLOJET
  - pp->H,W,Z
  - pp -> H+jet
  - pp -> Z+jet
  - pp -> 2 jets
  - ep -> 2jets
  - …

Single jet inclusive cross section

ATLAS jets

Theory setup

- NNPDF3.0_nnlo
- anti-k_T jet algorithm
- $\mu_R=\mu_F=\{p_{T1}, p_T\}$
- vary scales by factors of 2 and 1/2

Comparison to data

- ATLAS 7 TeV 4.5 fb^{-1}
- R=0.4

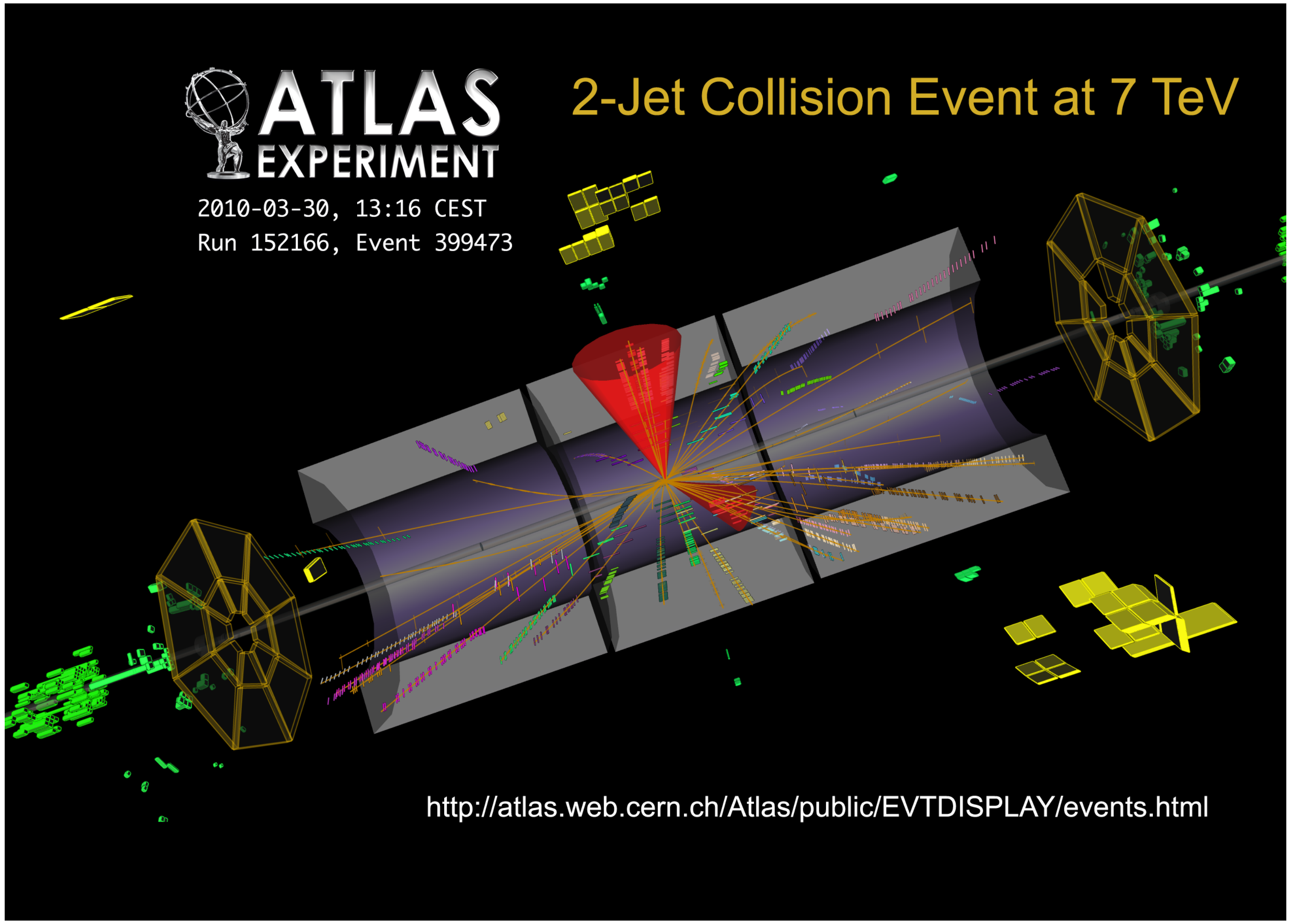

Ratio to NLO

- asymmetric scale band variation
- underestimated at small pT due to turn over of the NLO coefficient
- 20% uncertainty for central high pT jets rising to 40% for forward jets

Comparison to data

- non perturbative effects < 2% effect [JHEP 1509, 141 (2015)]
- data favours the pT1 scale choice at NLO

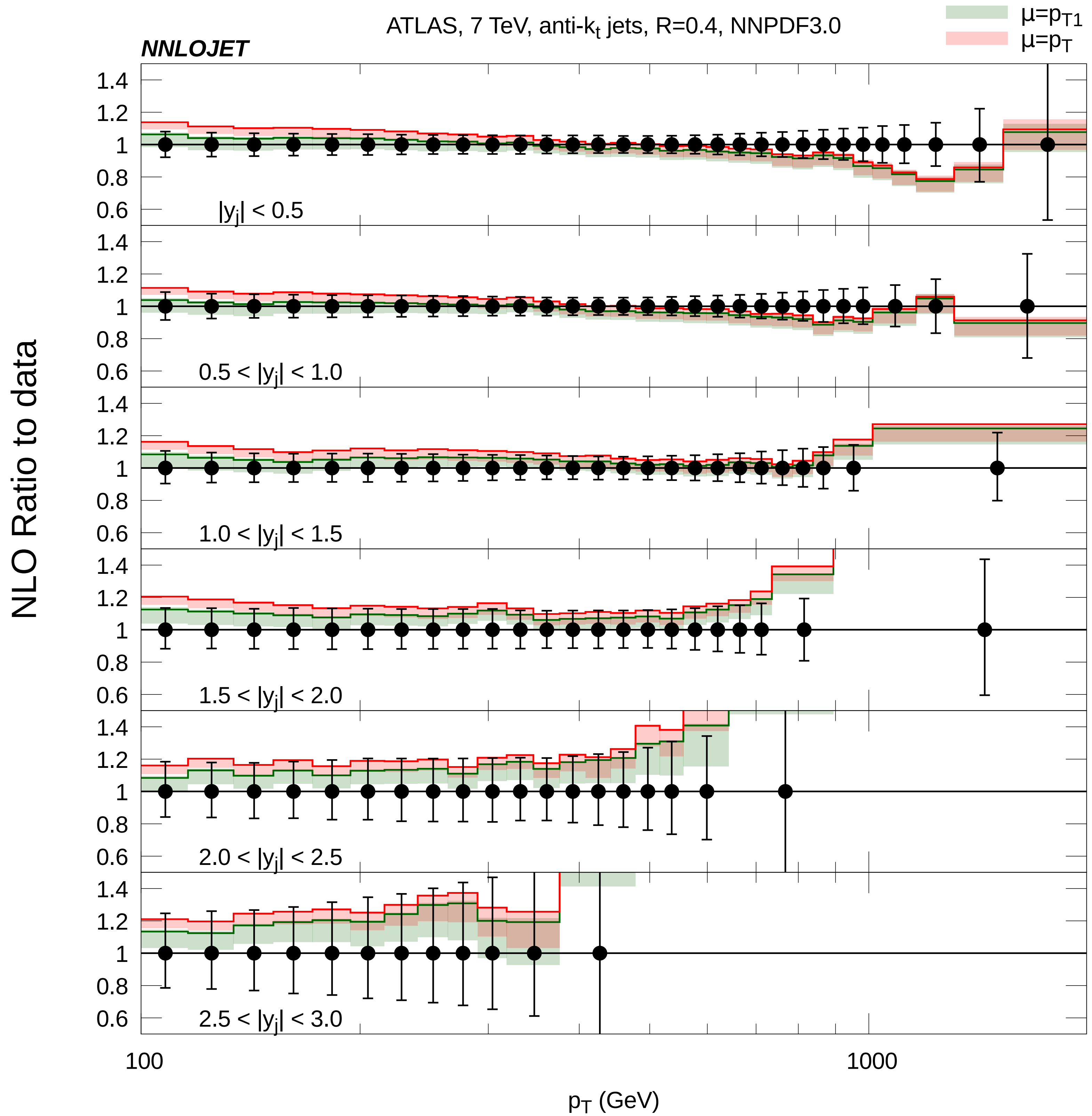

Ratio to NNLO

- symmetric scale band variation
- pT1!=pT effects enlarged at NNLO
- 10% scale uncertainty at low pT and percent level scale uncertainty at high pT

Comparison to data

- data favours the pT scale choice at NNLO

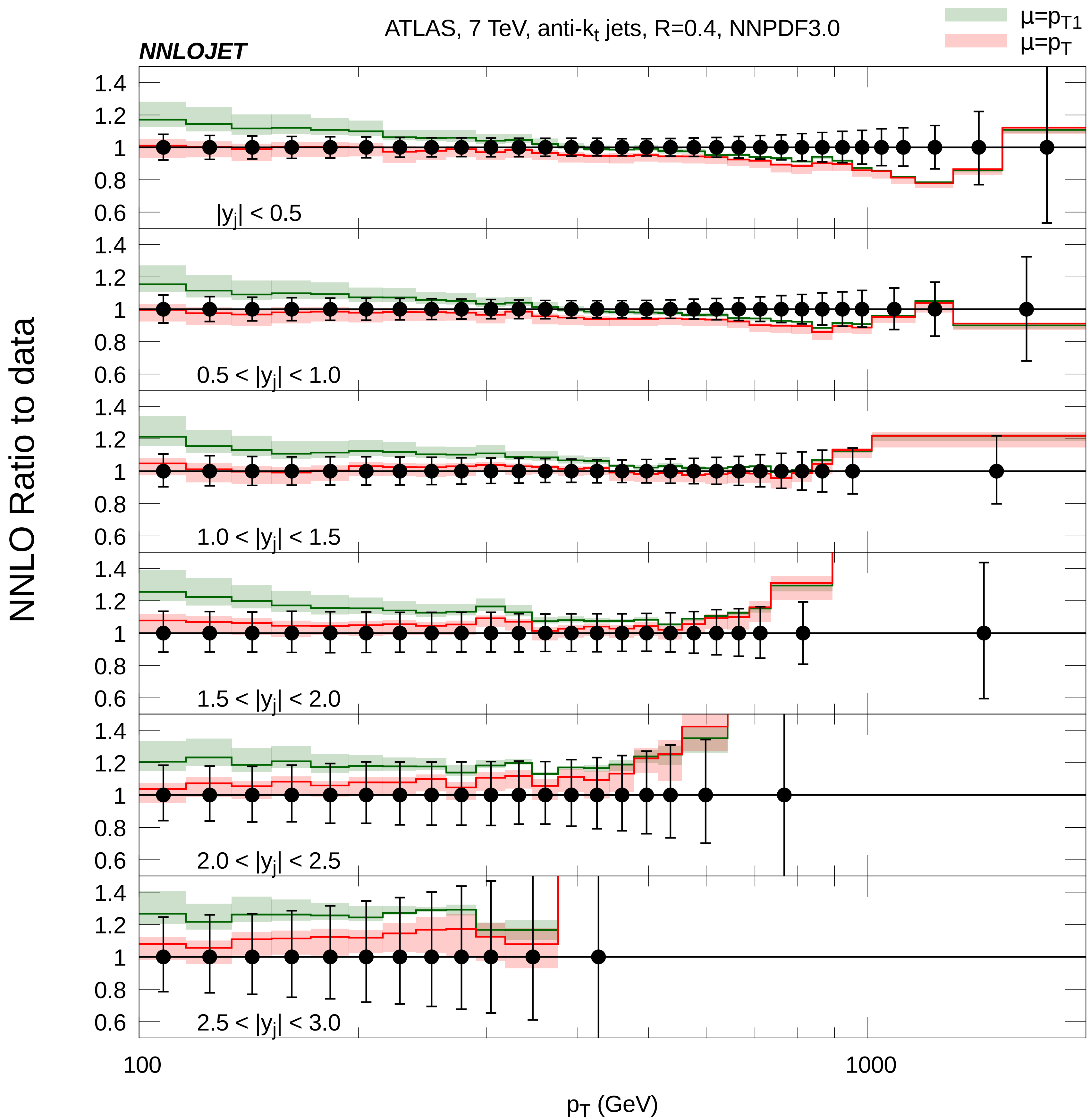

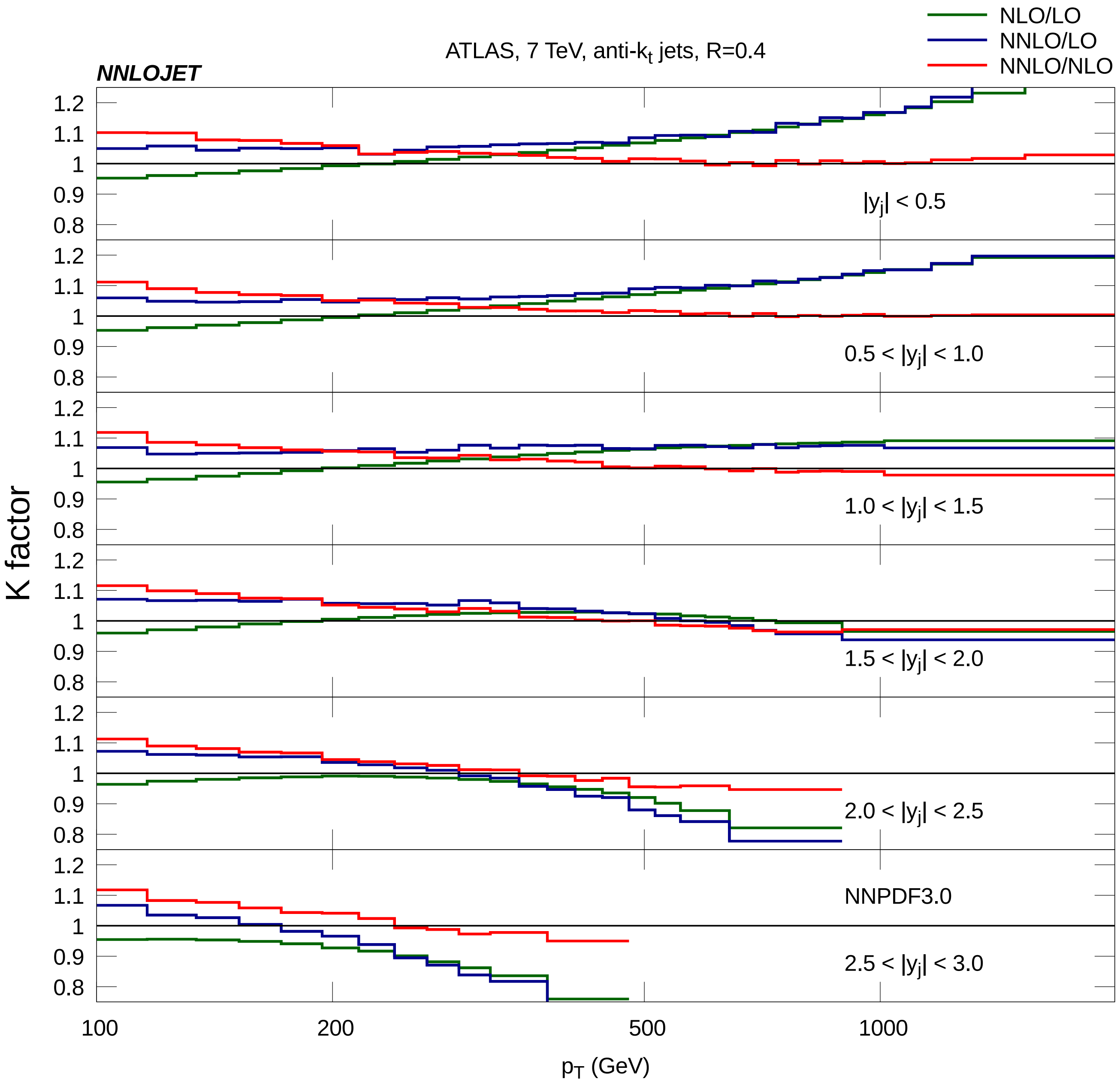

$$\mu_R = \mu_F = p_{T1}$$

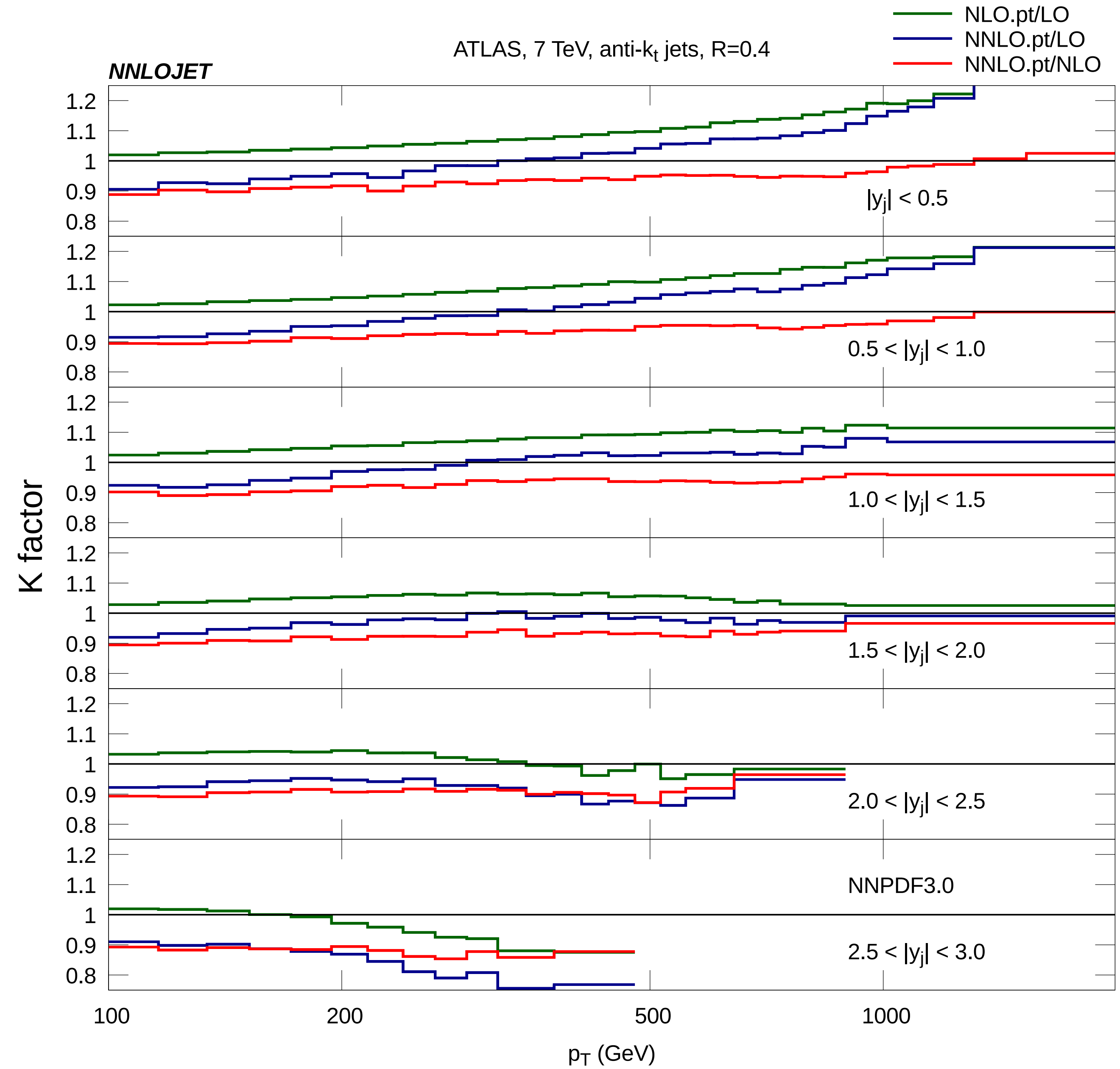

$$\mu_R = \mu_F = p_T$$

- NNLO effects around +10% at low pT and small at high pT
- Shape of NNLO/NLO k-factor is getting steeper going to the forward rapidity slices

- NNLO effects around -10% at low pT and small at high pT
- Shape of NNLO/NLO k-factor is getting flatter going to the forward rapidity slices

- Scale choice has a potential interplay with consistent fit of jet data in PDF's for all rapidity slices

Scale variation

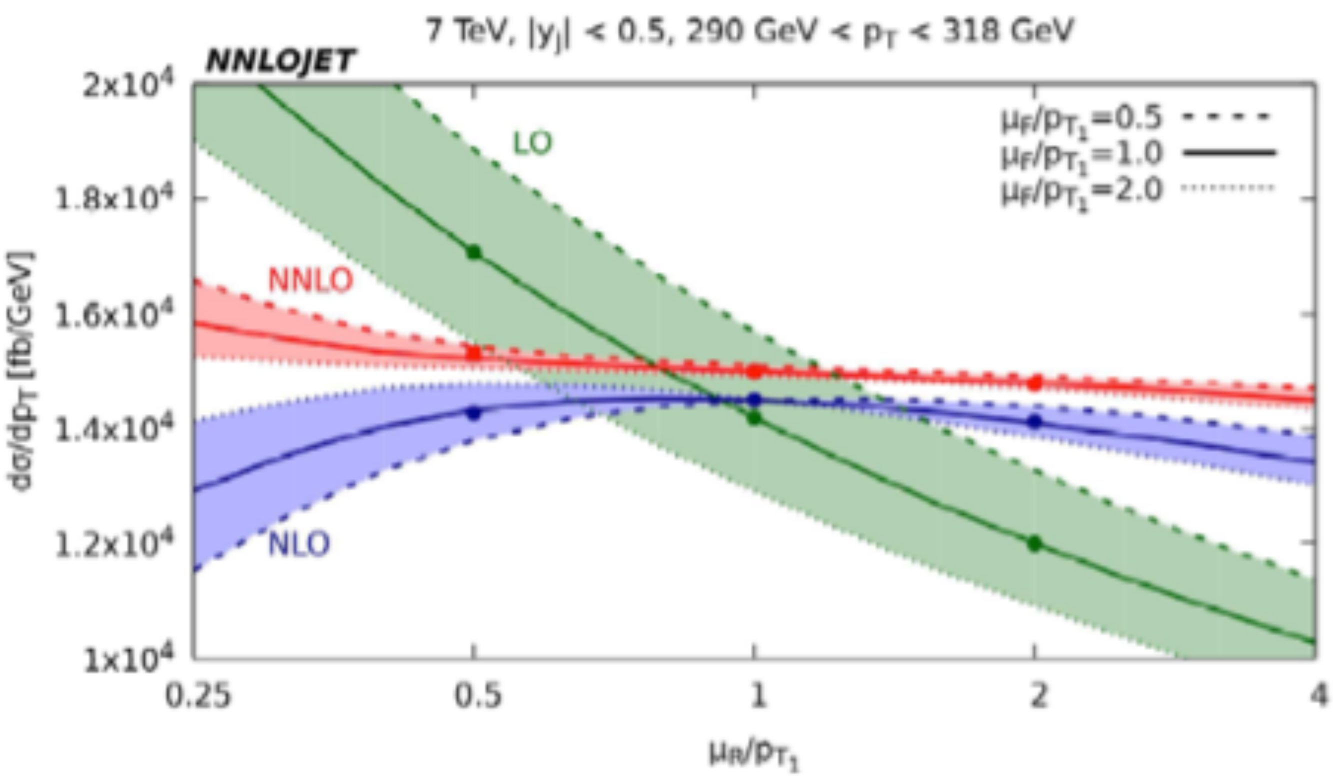

$$\mu_R = \mu_F = p_{T1}$$

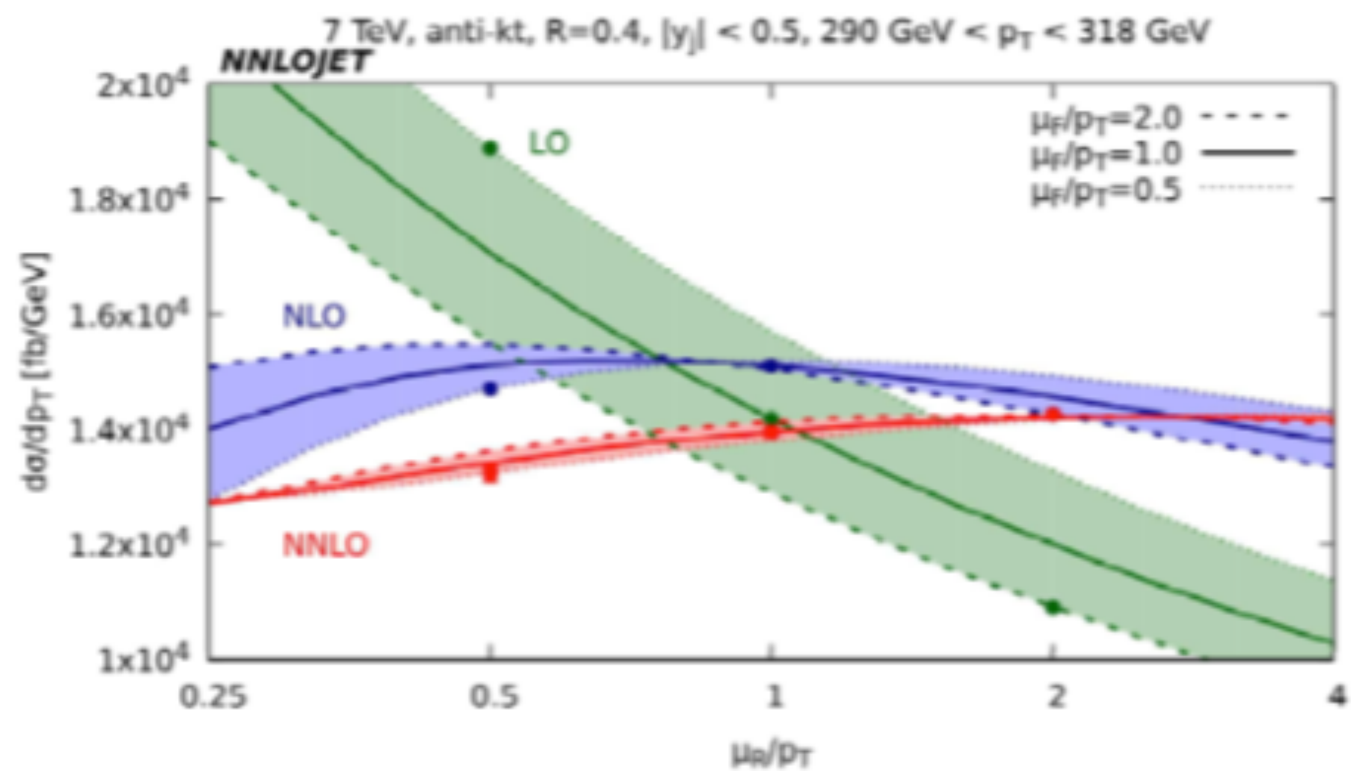

$$\mu_R = \mu_F = p_T$$

- Different behaviour in the NNLO scale variation
- Scale uncertainty much smaller than the difference between the two scale choices
- Difference in the prediction with either scale choice is beyond the scale variation uncertainty
- Lack of a theoretically well motivated preference motivates further study of this issue

Dijet inclusive cross section

ATLAS jets

Theory setup

- MMHT2014 nnlo
- anti-k_T jet algorithm
- p_{T1}>100 GeV; p_{T2}>50 GeV;
- $|y_{j1}|$, $|y_{j2}| < 3.0$
- $\mu_R = \mu_F = \{m_{jj}, \langle p_T \rangle\}$
- vary scales by factors of 2 and 1/2

Comparison to data

- ATLAS 7 TeV 4.5 fb^{-1}
- R=0.4

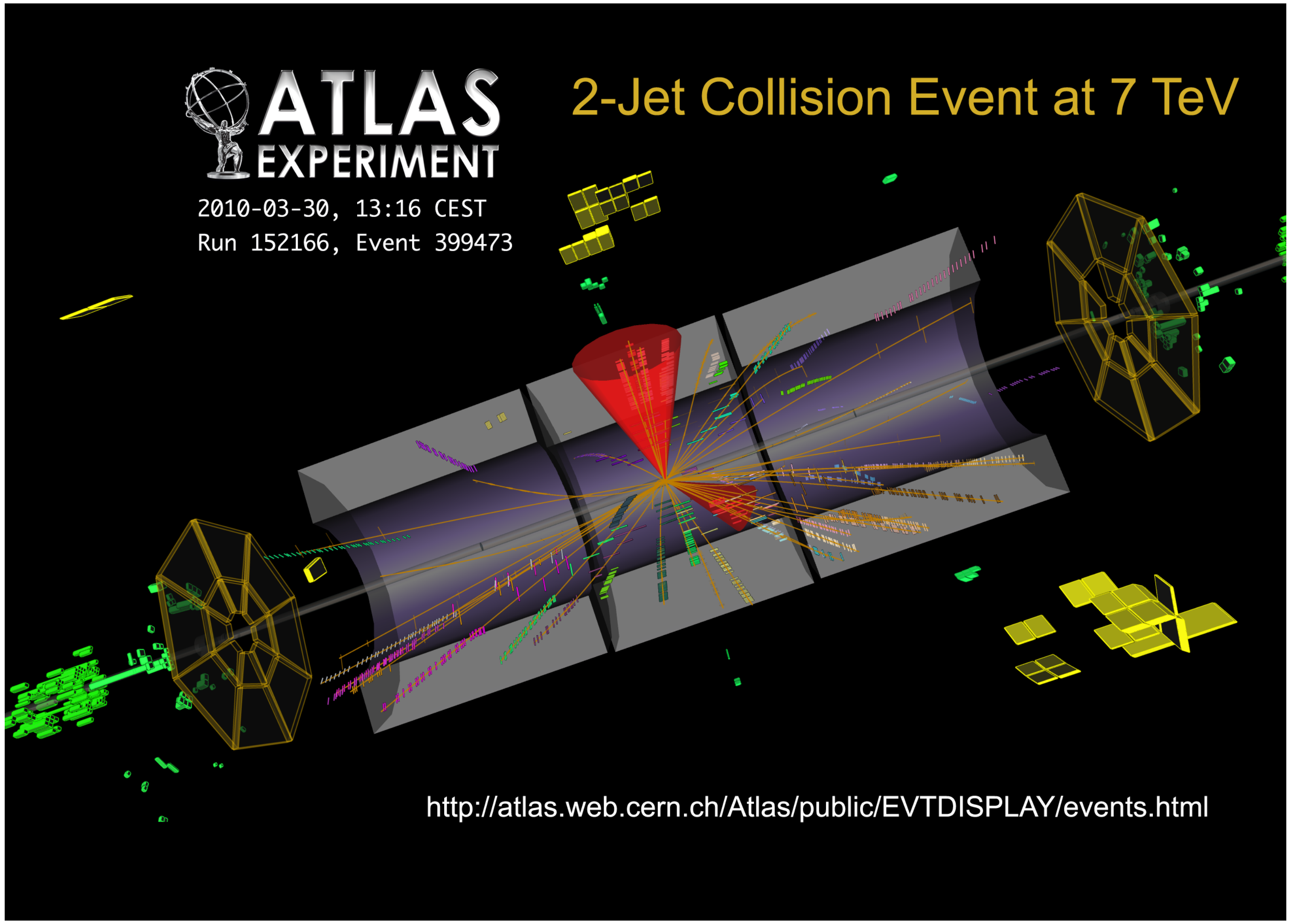

$$m_{jj}^2 = (p_{j1} + p_{j2})^2$$

$$y^* = \frac{1}{2}(y_{j1} - y_{j2})$$

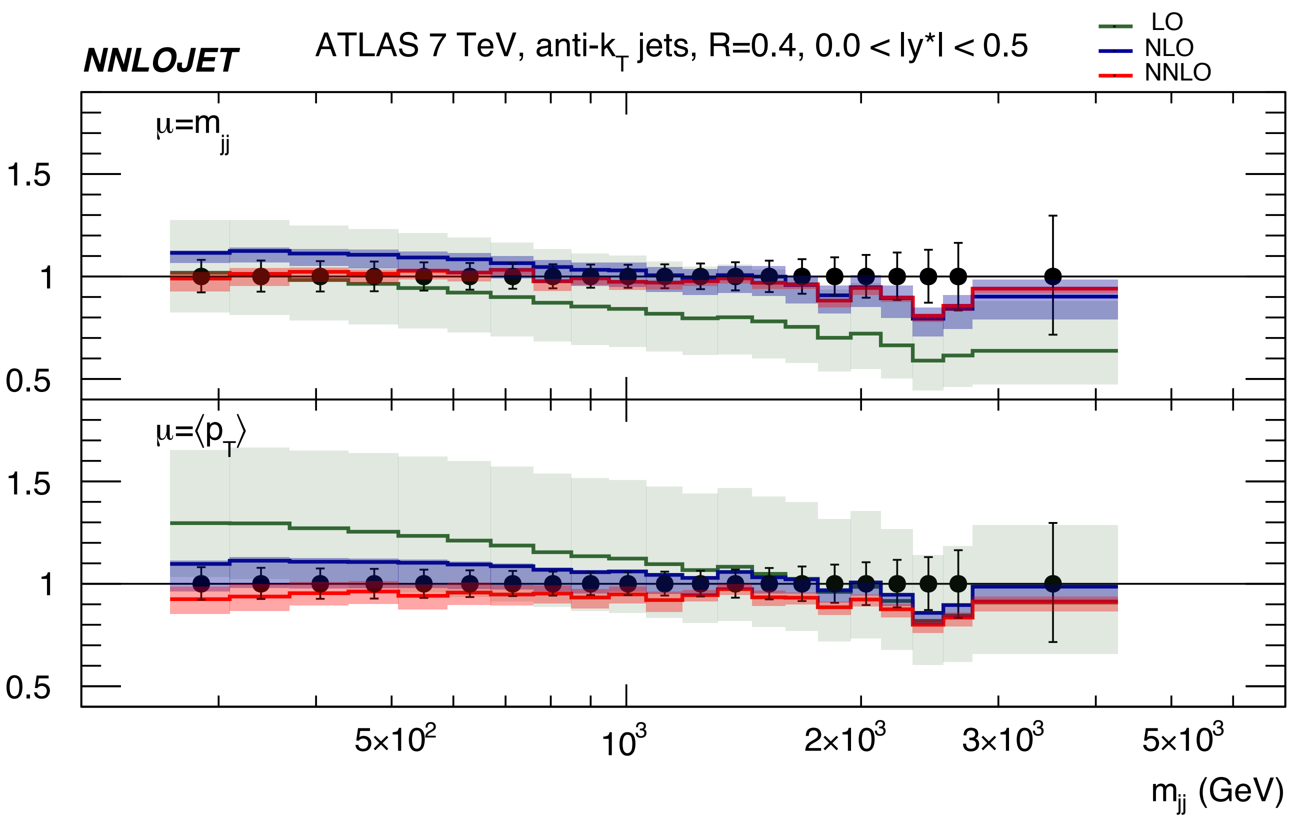

$0.0 < |y^*| < 0.5$

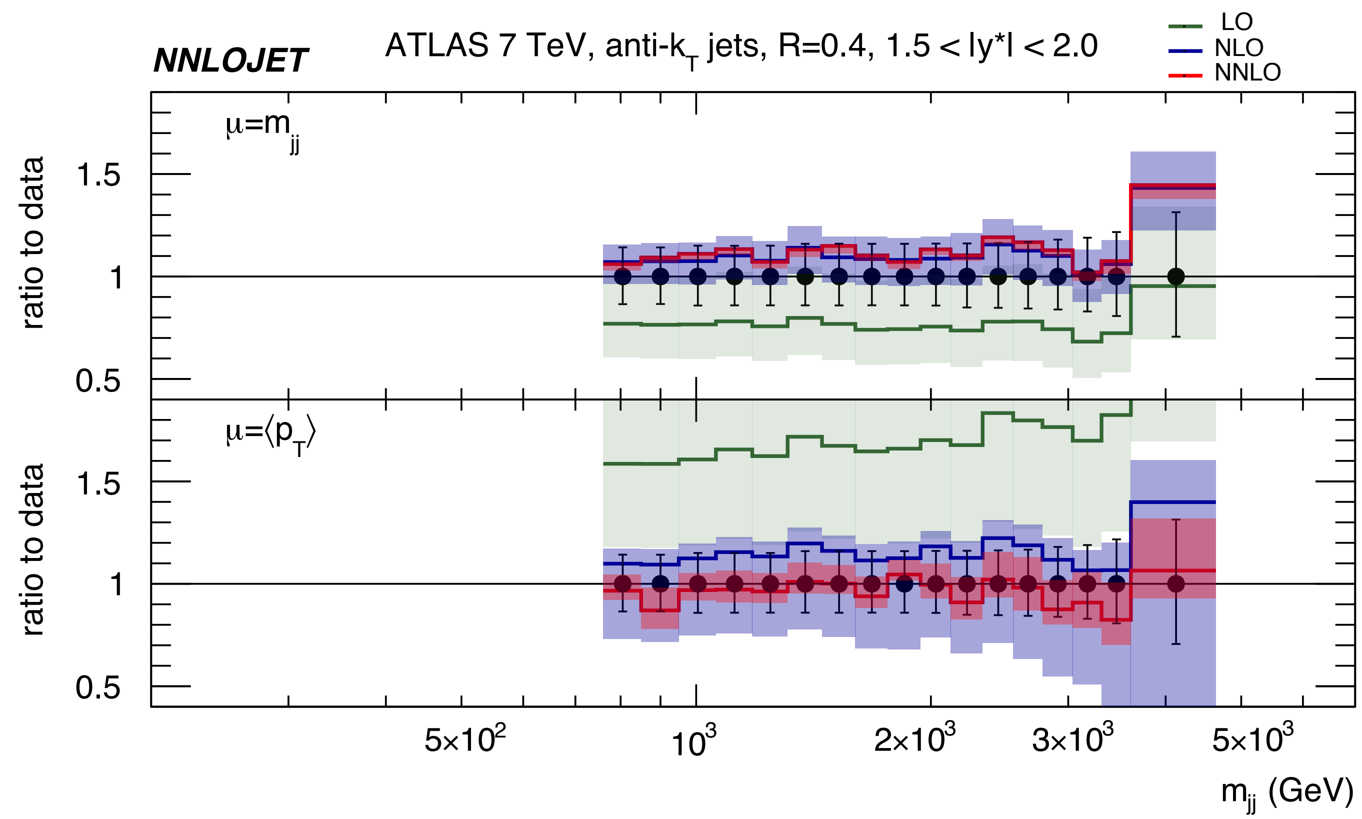

$1.5 < |y^*| < 2.0$

- Largely overlapping scale bands at small y* with either scale choice
- At large y* we observe with μ=<P$_T$> large negative NLO corrections, non-overlapping scale bands and residual NLO,NNLO scale uncertainty of ~100%,~20%
- Good theoretical motivation to use μ=m$_{jj}$ as central scale choice

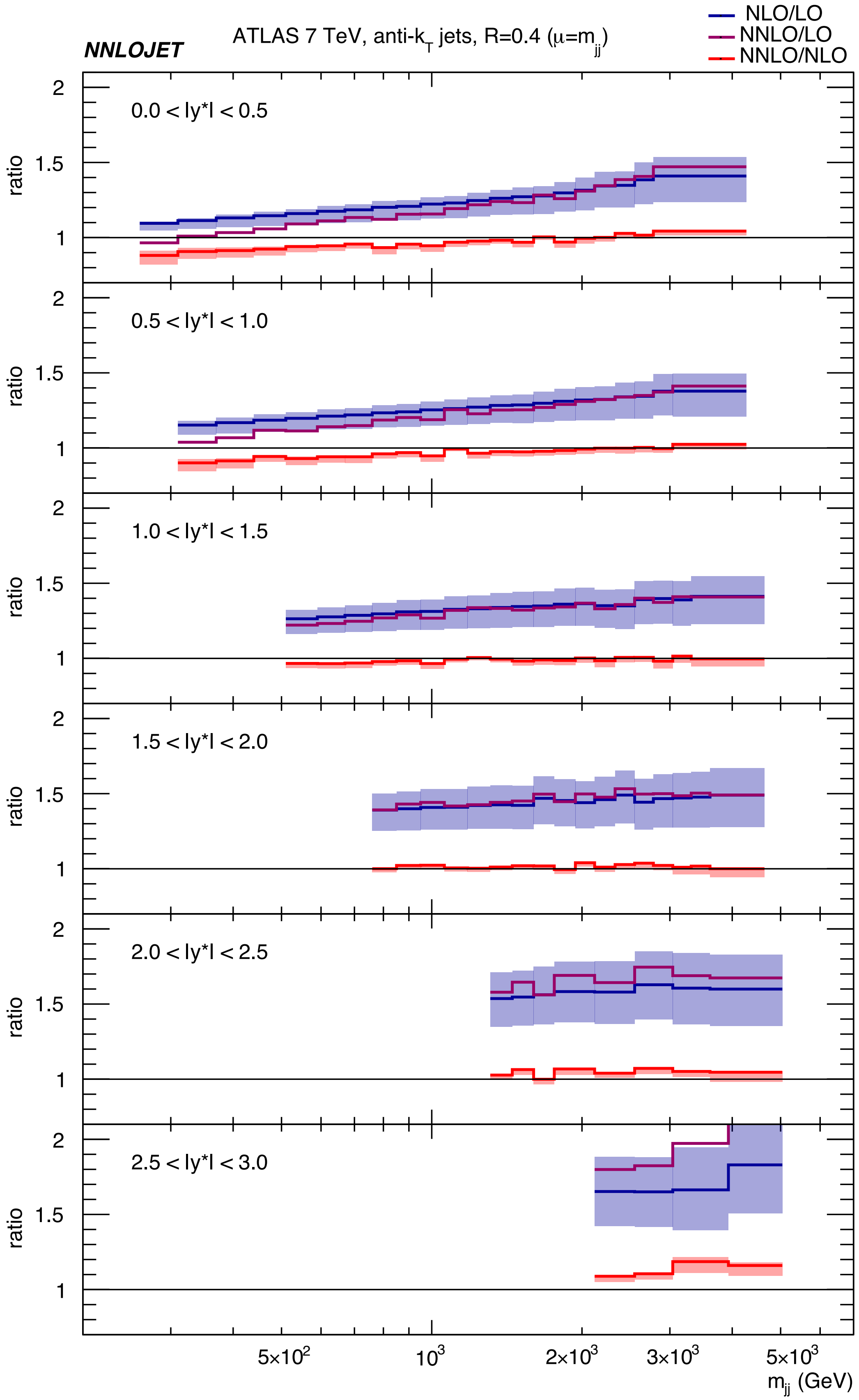

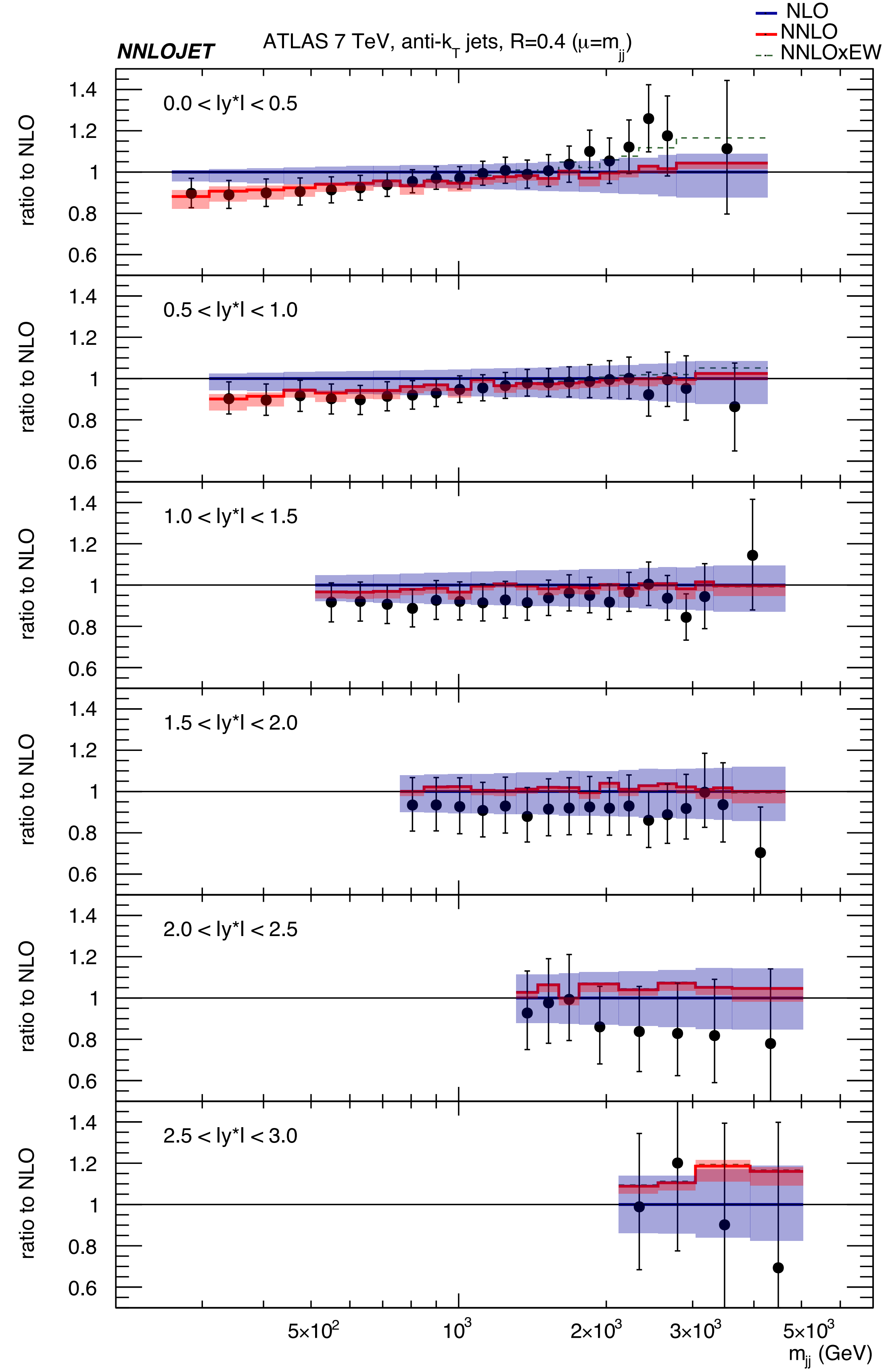

- Excellent convergence of the perturbative expansion; NNLO/NLO < 10% and flat
- Improved description of the dijet data at NNLO

Scale variation

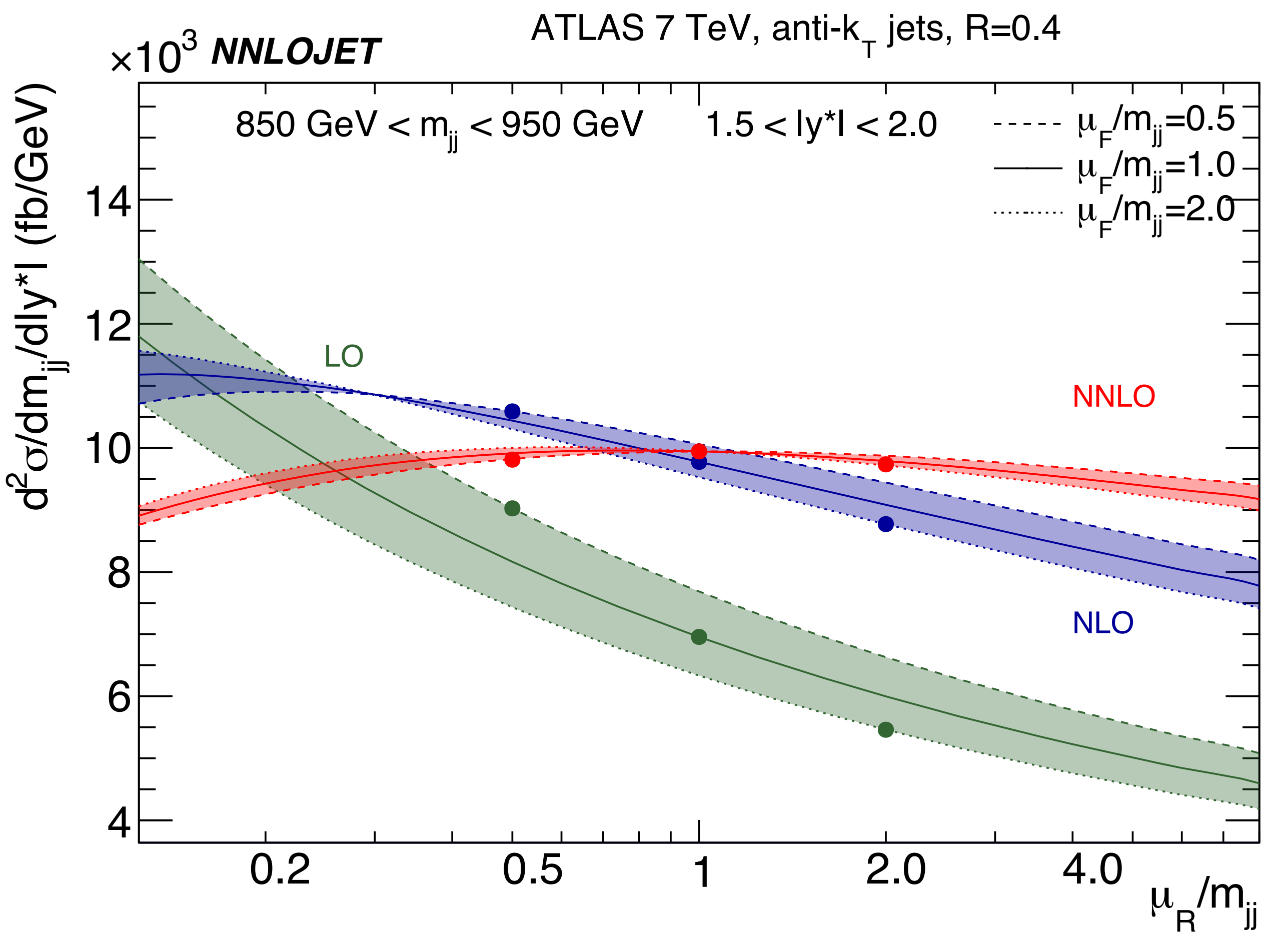

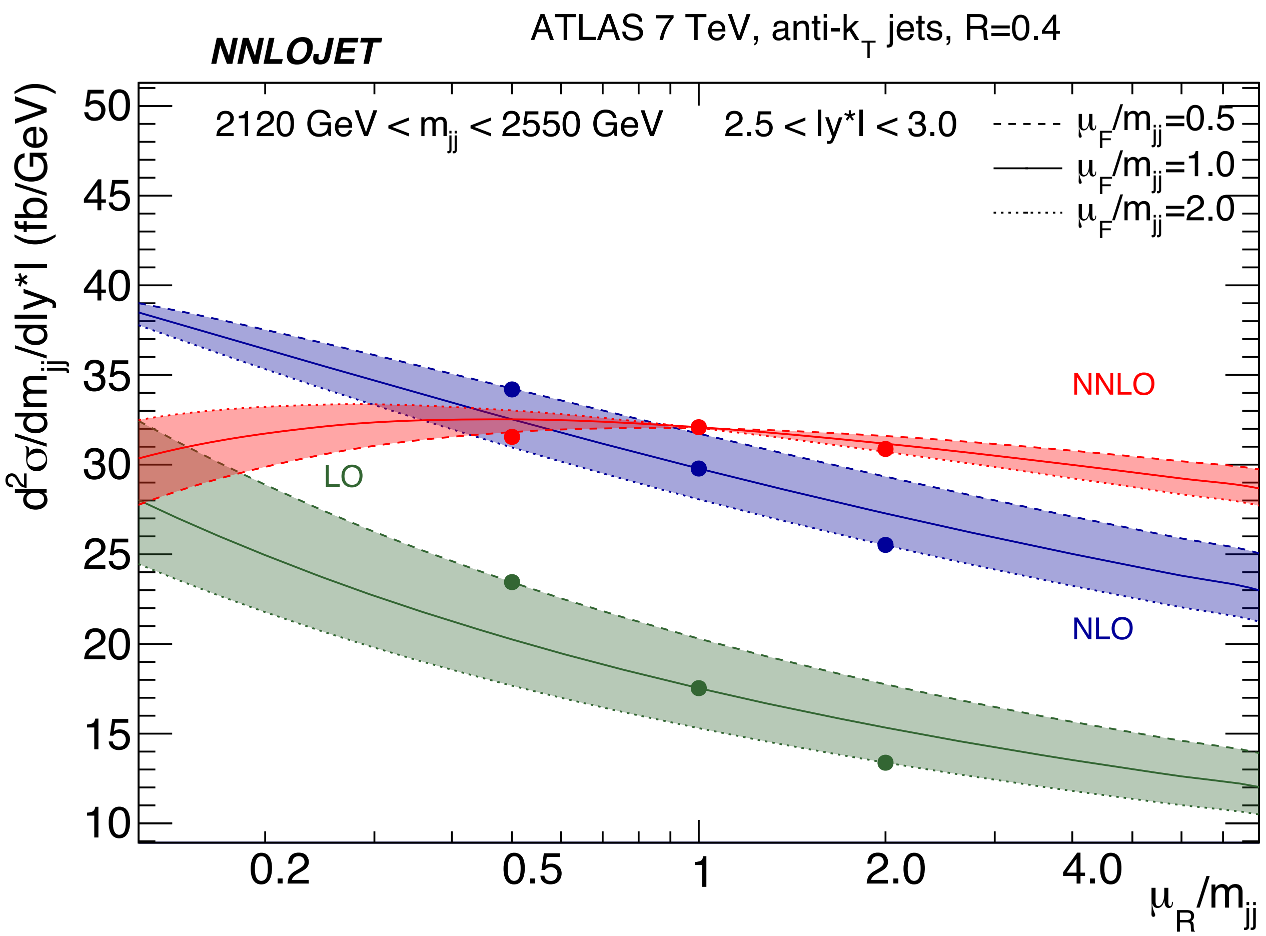

- Overlapping NLO and NNLO scale bands
- Significant reduction in scale dependence of the prediction at NNLO
- Residual scale uncertainty <5% smaller than experimental uncertainty on the observable

Conclusions

Substancial progress in NNLO calculations in past couple of years

- several different approaches for isolating IR singularities
- several new calculations available

<u>Antenna subtraction</u>

- local IR phase space subtraction scheme with analytic pole cancellation
- RR, RV, VV contributions separately finite and integrable in d=4
- formalism implemented in a fully flexible parton level generator
- new processes can be added using the existing common syntax structures
- distribution of results via applfast interface (to APPLGRID and fastNLO)

M. Sutton and K. Rabbertz tomorrow afternoon

BACKUP

Single jet inclusive scale choice

two widely used scale choices:

- $\mu_R = \mu_F = \{p_{T1}, p_T\}$
  - leading jet p_T in the event p_{T1}
  - individual jet p_T
- high p_T jets are back to back $\Rightarrow p_T \longrightarrow p_{T1}$

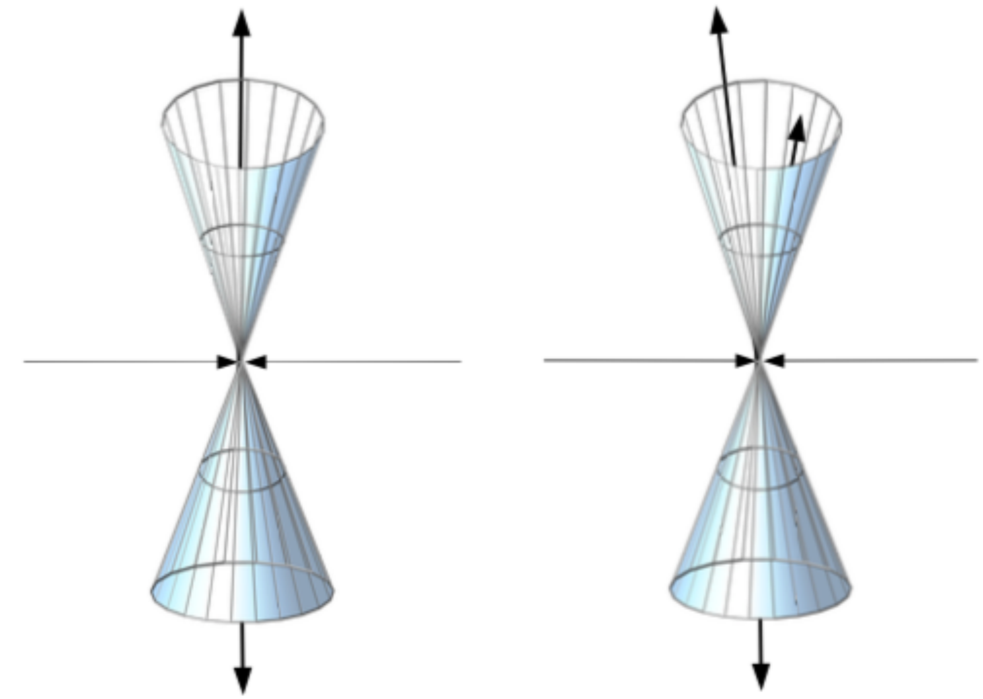

Single jet inclusive scale choice

two widely used scale choices:

- $\mu_R=\mu_F=\{p_{T1}, p_T\}$
    - leading jet p_T in the event p_{T1}
    - individual jet p_T
- high p_T jets are back to back ⇒ $p_T \longrightarrow p_{T1}$
- $p_T != p_{T1}$ for:
    - 3jet events
    - 3rd jet outside fiducial jet cuts

  ⇒ with p_T choice the real emission event with different R gives rise to a different scale ⇒ larger R ⇒ harder scale ⇒ $p_T \longrightarrow p_{T1}$
- at NLO the p_{T1} scale choice generates the same hard scale for the event independent of the value of R